The all-seeing eye of resonant Auger electron spectroscopy: a study on aqueous KCl

Tsveta Miteva,[*,†] Nikolai V. Kryzhevoi,[‡] Nicolas Sisourat,[†] Christophe Nicolas,[¶] Wandared Pokapanich,[§] Thanit Saisopa,[‖] Prayoon Songsiriritthigul,[‖] Yuttakarn Rattanachai,[⊥] Andreas Dreuw,[#] Jan Wenzel,[#] Jérôme Palaudoux,[†] Gunnar Öhrwall,[@] Ralph Püttner,[△] Lorenz S. Cederbaum,[‡] Jean-Pascal Rueff,[†,¶] and Denis Céolin[*,¶]

†*Sorbonne Université, CNRS, Laboratoire de Chimie Physique Matière et Rayonnement, UMR 7614, F-75005 Paris, France*

‡*Theoretische Chemie, Physikalisch-Chemisches Institut, Universität Heidelberg, Im Neuenheimer Feld 229, D-69120 Heidelberg, Germany*

¶*Synchrotron SOLEIL, l'Orme des Merisiers, Saint-Aubin, F-91192 Gif-sur-Yvette Cedex, France*

§*Faculty of Science, Nakhon Phanom University, Nakhon Phanom 48000, Thailand*

‖*School of Physics, Suranaree University of Technology, Nakhon Ratchasima 30000, Thailand*

⊥*Department of Applied Physics, Faculty of Sciences and Liberal Arts, Rajamangala University of Technology Isan, Nakhon Ratchasima 30000, Thailand*

#*Interdisciplinary Center for Scientific Computing, Ruprecht-Karls University, Im Neuenheimer Feld 205A, D-69120 Heidelberg, Germany*

@*MAX IV Laboratory, Lund University, P.O. Box 118, SE-22100 Lund, Sweden*

△*Fachbereich Physik, Freie Universität Berlin, Arnimallee 14, D-14195, Berlin, Germany*

E-mail: tsveta.miteva@upmc.fr; denis.ceolin@synchrotron-soleil.fr

Methods

Experimental set-up

A differentially-pumped tube in which the microjet head is inserted, is mounted on a 3-axes motorized manipulator in front of the spectrometer lens. Two holes of 2 mm diameter allow the photons to go in and out. At the end of the tube and in front of the lens, a 500 μm diameter hole skimmer allows the electrons created at the interaction point to go in the direction of the spectrometer. The microjet head is mostly composed of a 30 μm diameter vertical glass capillary facing a temperature-controlled catcher in CuBe having a 300 μm hole, and a camera. Piezo motors allow their precise alignment relative to each other and to the photon beam. The catcher is placed at a distance of about 5 mm from the capillary and is permanently pumped in order to extract the liquid. For the present experiment, a 0.5M KCl aqueous solution is injected in the capillary by a high performance liquid chromatography (HPLC) pump with a constant flux of 1.6 ml/min. The alignment of the setup is performed on the KCl aqueous solution by measuring the water O1s XPS peak intensity and by optimizing the liquid vs gas phase ratio. The pressure in the main chamber is kept below the 10^{-5} mbar range whereas it is kept at about 10^{-4} mbar in the differentially-pumped tube when the HPLC pump is ON. Our equipment is an updated version of the equipment used in Ref.[1]

Ab initio calculations

In order to obtain realistic structures corresponding to the bulk solution, we carried out constrained geometry optimization starting from the equilibrium gas-phase geometry[2,3] and then fixing the K-O distance to 2.840 Å and increasing the angle θ between the K-O bond and the C_3 axis to 55° such that these parameters correspond to other theoretical and experimental works[4,5].

We analyzed the core excited states by expanding the natural orbitals occupied by the

excited electron (singly occupied natural orbitals, SONOs) ψ_i of the microsolvated clusters in the basis of SONOs of the bare K^+ or Cl^- ion χ_{nl}

$$\psi_i = \sum_{nl} a^i_{nl} \chi_{nl} \tag{1}$$

where n and l stand for the principal and orbital quantum numbers as described in Ref.[6]. The expansion coefficients a^i_{nl} show the degree of delocalization of the excited electron and the mixing of the core excited states in the ligand field created by the surrounding water molecules (see Fig. 4).

Core-excited states of Cl^-

The intensity of the $Cl^-(1s^{-1}4p)$ state is lower than that of the $Cl^-(1s^{-1}5p)$ state contrary to what is observed in K^+. This difference can be explained by the lower electron density of the 4p compared to the 5p electron in the region close to the core hole which thus results in the lower oscillator strength of the $1s^{-1}4p$ compared to the $1s^{-1}5p$ transition in Cl^- (see Fig. 1). In what follows we give a simple explanation of the difference in the radial density distributions of the $1s^{-1}4p$ and $1s^{-1}5p$ states in K^+ and Cl^-. In the case of K^+, the excited electron mainly sees a $2/r$ potential. In addition, it sees a short range potential originating from the point-like nucleus and the screening electrons. The influence of the latter can be described by a quantum defect $\delta \neq 0$, which is almost constant for the entire infinite Rydberg series. However, in case of Cl^- the outer electron does not experience a Coulomb potential and the short range potential becomes dominant. As a result of the absence of the Coulomb potential we see a different behavior in the properties of the states, like e.g. only a finite number of bound states (here obviously 4p)[7]. In contrast to this, the 3d and 5p states are not bound.

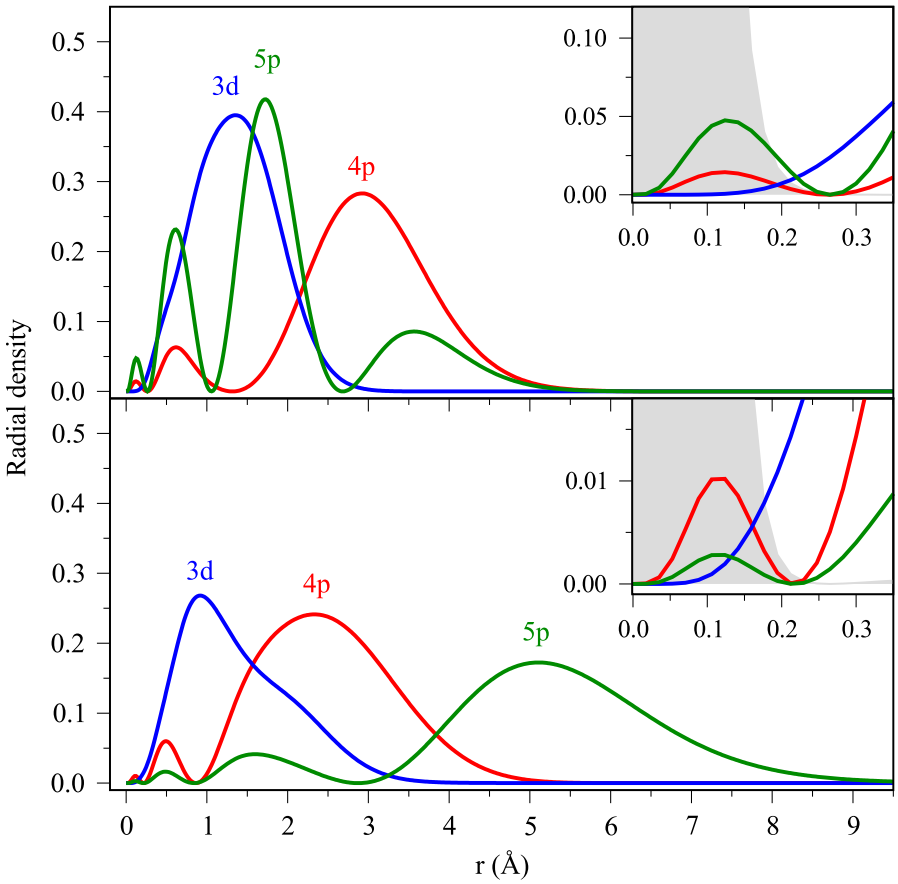

Figure 1: Radial density distributions of the singly-occupied natural orbital occupied by the excited electron corresponding to the $1s^{-1}4p$, $1s^{-1}3d$ and $1s^{-1}5p$ core excitations in K^+ (lower panel) and Cl^- (upper panel). The insets show the region of distances relevant for the overlap with the 1s core orbital whose radial density is shown as a grey shaded area.

References

(1) Faubel, M.; Schlemmer, S.; Toennies, J. P. A molecular beam study of the evaporation of water from a liquid jet. *Z. Phys. D* **1988**, *10*, 269–277.

(2) Lee, H. M.; Kim, J.; Lee, S.; Mhin, B. J.; Kim, K. S. Aqua-potassium(I) complexes: Ab initio study. *J. Chem. Phys.* **1999**, *111*, 3995–4004.

(3) Lee, H. M.; Kim, D.; Kim, K. S. Structures, spectra, and electronic properties of halide-water pentamers and hexamers, $X^-(H_2O)_{5,6}$ (X=F,Cl,Br,I): Ab initio study. *J. Chem. Phys.* **2002**, *116*, 5509–5520.

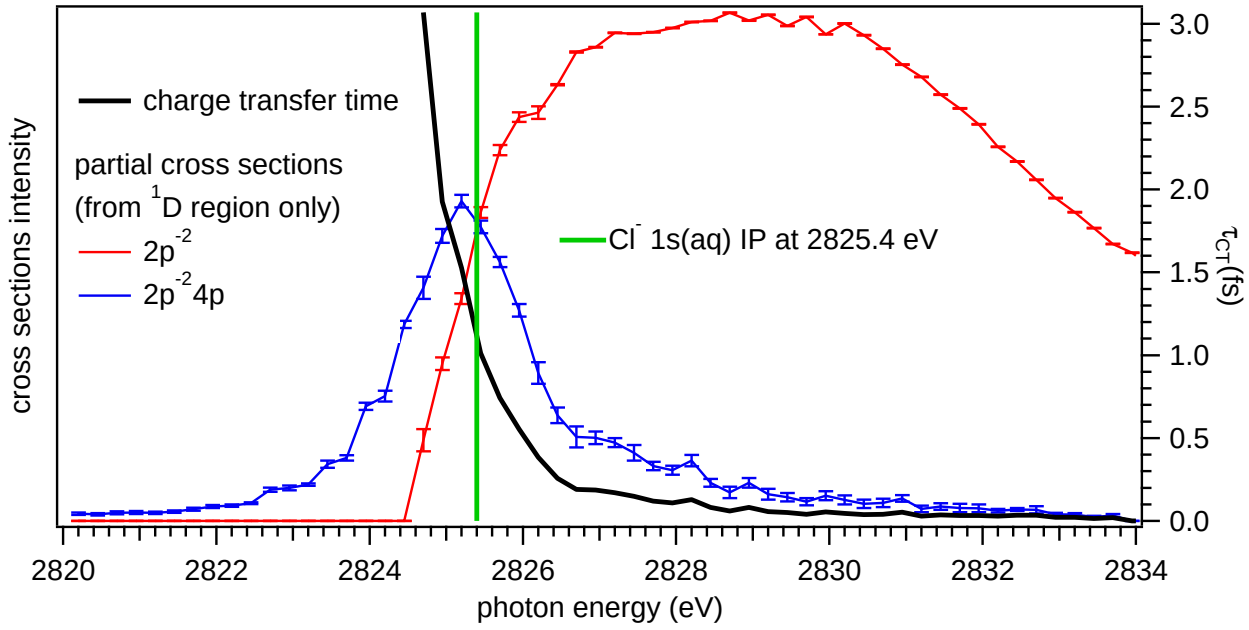

Figure 2: Partial cross sections and charge transfer time extracted from Fig. 3. The blue and red curves are obtained by integrating the area of the $2p^{-2}$ and $2p^{-2}4p$ final states (^{1}D state region only) at each photon energy step. From these curves we determine the charge transfer time τ_{CT} according to the formula $\tau_{\mathrm{CT}} = \tau_c l/d$, with τ_c being the Cl 1s core-hole lifetime and l/d being the intensity ratio of the localized ($2p^{-2}4p$) and delocalized ($2p^{-2}$) states at a given excitation energy.[8] The green line defines the $Cl^-_{aq}(1s)$ ionization potential.

(4) Ma, H. Hydration structure of Na^+, K^+, F^-, and Cl^- in ambient and supercritical water: A quantum mechanics/molecular mechanics study. *Int. J. Quant. Chem.* **2014**, *114*, 1006–1011.

(5) Ohtaki, H.; Radnai, T. Structure and dynamics of hydrated ions. *Chem. Rev.* **1993**, *93*, 1157–1204.

(6) Miteva, T.; Wenzel, J.; Klaiman, S.; Dreuw, A.; Gokhberg, K. X-Ray absorption spectra of microsolvated metal cations. *Phys. Chem. Chem. Phys.* **2016**, *18*, 16671–16681.

(7) Buckman, S. J.; Clark, C. W. Atomic negative-ion resonances. *Rev. Mod. Phys.* **1994**, *66*, 539–655.

(8) Föhlisch, A.; Feulner, P.; Hennies, F.; Fink, A.; Menzel, D.; Sanchez-Portal, D.; Echenique, P. M.; Wurth, W. Direct observation of electron dynamics in the attosecond domain. *Nature* **2005**, *436*, 373.